Predicted Performance Effects of Blade Elasticity on Testing of Rotors for Mars

Stephen J. Wright
Aerospace Engineer
NASA Ames Research Center
Moffett Field, CA, USA

Witold J. F. Koning
Aerospace Engineer
Science and Technology Corporation
NASA Ames Research Center
Moffett Field, CA, USA

B. Natalia Perez Perez
Aerospace and Mechanical Engineer
Science and Technology Corporation
NASA Ames Research Center
Moffett Field, CA, USA

Haley V. Cummings
Mechanical Engineer
NASA Ames Research Center
Moffett Field, CA, USA

Wayne Johnson
Aerospace Engineer
NASA Ames Research Center
Moffett Field, CA, USA

ABSTRACT

The Rotor Optimization for the Advancement of Mars Exploration project (ROAMX) has designed and manufactured a set of rotor blades optimized for hover on Mars. These blades will soon be tested for hover performance in the NASA Ames Research Center Planetary Aeolian Laboratory, a large vacuum chamber capable of rotor testing at reduced pressures. To match the tip Mach numbers during this testing with the tip Mach numbers that would be experienced in the Martian atmosphere, the rotor will be spun faster in the vacuum chamber than it would be spun on Mars. While this accomplishes the goal of simulating the tip Mach numbers of Mars operations, the elevated RPM may have undesired consequences for performance, due to elastic deflections of the blades. The purpose of this paper is to use CAMRAD II, a rotorcraft comprehensive analysis code, to predict the effect on performance of blade elasticity at elevated RPM in the vacuum chamber environment. Results are presented for different thrust conditions and different rotor speeds, and comparisons are made between rigid and elastic blade predictions. Overall, the CAMRAD II analysis suggests that blade elasticity does influence rotor performance in the operating conditions of interest, although the effect is moderate enough to conclude that the PAL testing will be a good simulation of Mars operation.

NOMENCLATURE

A	disk area, m^2
c_{do}	mean drag coefficient, $8C_{Po}/\sigma$
FM	figure of merit, $P_m/(P_o + P_i)$
T	thrust, N
C_{Po}	profile power coefficient
C_T	thrust coefficient, $T/\rho A V_{tip}^2$
M_{tip}	tip Mach number
V_{tip}	tip speed, m/s
P_i	induced power, $kg \cdot m^2/s^3$
P_m	momentum theory power, $kg \cdot m^2/s^3$
P_o	profile power, $kg \cdot m^2/s^3$
ρ	density, kg/m^3
σ	thrust-weighted solidity

INTRODUCTION

The Rotor Optimization for the Advancement of Mars Exploration (ROAMX) project has investigated rotor blade design optimization for hovering flight on Mars (Ref. 1). An in-house code, Evolutionary Algorithm for Iterative Studies of Aeromechanics (ELISA) (Ref. 2), was used for optimization of the airfoils, planform, and twist distribution, and the University of Maryland (UMD) performed the structural design of the blades (Ref. 3). Figure 1 illustrates the geometry of the ROAMX rotor blade. A set of the optimized blades will soon be tested for hover performance in the NASA Ames Research Center Planetary Aeolian Laboratory (PAL), a large (4000 m^3) vacuum chamber capable of rotor testing at reduced pressures (Ref. 4).

During testing in the PAL, it is desired that both tip Mach number (M_{tip}) and Reynolds number match conditions that would be encountered on Mars. In the PAL, Earth's atmosphere at ambient temperatures results in a higher speed of sound than that in the cold, CO_2 atmosphere of Mars. Because of this difference, the rotor tip speed (V_{tip}) in the PAL must be ~1.46 times the V_{tip} on Mars to reach the same M_{tip}. Adjusting pressure in the PAL yields Reynolds numbers in the range of Martian operating conditions.

Presented at the VFS Autonomous VTOL Technical Meeting, Mesa, Arizona, USA Jan. 24-26, 2023.

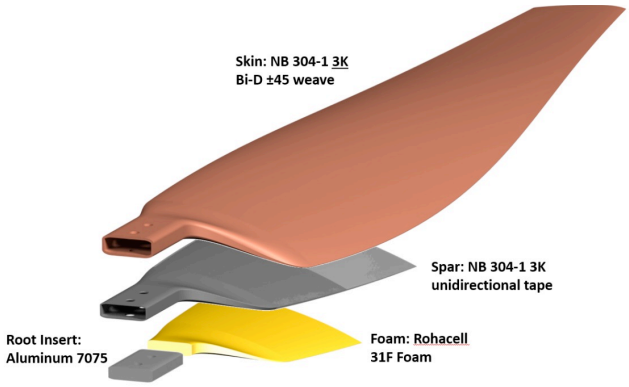

Figure 1. ROAMX blade geometry (Ref. 3)

While spinning the rotor faster on earth accomplishes the goal of simulating the M_{tip} values of Mars operations, there may be undesired performance effects of increasing RPM, due to the elastic deflections of the blades. As shown in Ref. 5 for Ingenuity, the use of 5% thick outboard airfoils achieves the high frequency of the low-damped regressive flap mode, required for sufficient control gain margin of the coaxial rotor cyclic control. However, the ROAMX rotor will be experimentally tested in a single rotor configuration with only collective control, so the required coning mode frequency can be obtained using thinner airfoil sections. The ROAMX rotor achieves significant performance gains by using 1% thick outboard airfoils, resulting in relatively soft blades. High RPM increases inertial loads which may result in levels of elastic deformation that affect the performance of the rotor.

The purpose of this paper is to use CAMRAD II (Ref. 6), a rotorcraft comprehensive analysis code, to computationally predict the effect on performance of blade elasticity at high RPM in the PAL environment. Specifically, this work investigates to what extent blade elasticity must be considered when attempting to simulate low-RPM/high-Mach-number operation on Mars with high-RPM/matched-Mach-number operation on earth.

MODELING AND ANALYSIS

The analysis in this work is accomplished with CAMRAD II. Key parameters of the CAMRAD II model are presented in Table 1.

Table 1. CAMRAD II Rotor Model Parameters

Parameter	Value
Number of blades	4
Thrust-weighted solidity	0.16548
Radius (m)	0.720

CAMRAD II is capable of both rigid and elastic blade analysis. For the latter, the program requires sectional structural properties for the blades. Sectional inertial properties are needed, as well as section stiffnesses in the extensional (EA), flap (EIFLAP), lag (EILAG), and torsional (GJ) degrees of freedom. As discussed in Ref. 3, the ROAMX blades are quite unconventional, with no spar and a 1% thickness to chord ratio outboard of 50% radius.

For the present work, the IXGEN/VABS (Ref. 7) modeling and analysis tool was used to determine the inertial properties. The chordwise center of gravity was adjusted to be located at 50% chord, in accordance with UMD's structural analysis (Ref. 3).

An attempt was made to use IXGEN/VABS to determine EIFLAP, EILAG, and GJ. However, this modelling effort yielded values deemed unrealistic. In lieu of the VABS results for EIFLAP, EILAG, and GJ, an approximate distribution was developed for these three parameters. The starting point for the radial distribution of stiffnesses was the VABS output. Modifications were made to this distribution to approximately match the modal frequencies across a range of rotor speeds with those previously predicted by the University of Maryland via X3D (Ref. 3). A fan plot generated with the CAMRAD II model is presented in Fig. 2. The fan plot was generated with vacuum conditions with nominal collective pitch of 18.5 degrees. The blade is very soft in torsion, particularly for the outboard section of the blade which is 1% thick and does not have a spar. Thus, it is unsurprising that the CAMRAD II analysis shows the blade's second mode to contain a significant amount of torsional motion. CAMRAD II's prediction of the second mode being a low frequency torsion mode was supported by a resonance assessment profile test of the manufactured blade.

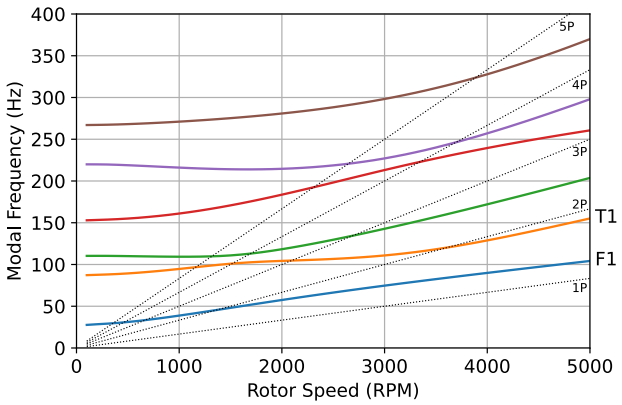

Figure 2. Modal frequency vs rotor speed. Vacuum conditions with 18.5 degree collective

For the aerodynamics in the simulations, CAMRAD II free wake analysis was used. The airfoil lookup tables were those developed by the ROAMX project using OVERFLOW (Ref. 2).

The environmental conditions for the PAL analysis are tabulated in Table 2, alongside corresponding values for a Mars environment. Key parameters include density, viscosity, and speed of sound. The density and temperature on Mars are the design operating conditions. The temperature in the PAL is ambient, and the density is chosen to match Reynolds number.

Table 2. PAL and Mars Environment Parameters

Parameter	PAL	Mars
Density (kg/m^3)	0.0151	0.0170
Viscosity (N·s/m^2)	1.75 10^{-5}	1.13 10^{-5}
Speed of sound (m/s)	340.91	233.13
Temperature (degrees C)	16.04	-50
Reynolds number at 75% radius and M_{tip} = 0.80	17877	17900

RESULTS

Collective Pitch Sweeps

The results of this sub-section are collective sweeps in hover of the ROAMX rotor with the PAL environment at different values of M_{tip}. Collective was swept from 0 degrees to 24 degrees (values at 75% radius). The same types of plots are shown for four different values of M_{tip}: 0.70, 0.80, 0.90, and 0.95.

The rotor design blade loading is $C_T/\sigma = 0.115$, corresponding to collective pitch of about 10 deg. With 50% thrust increase for control, expected peak power is at about $C_T/\sigma = 0.17$. The ROAMX rotor geometry (airfoil sections, twist, chord distribution for fixed thrust-weighted solidity) were optimized for $C_T/\sigma = 0.175$ (corresponding to about 18.5 deg collective), giving good performance at both design blade loading and stalled conditions.

Figures 3-5 are from analysis with M_{tip} of 0.70. Figure 3 is a plot of C_T/σ vs input rotor collective pitch for both rigid and elastic blade analyses. From 0 degrees to nearly 20 degrees collective, the rigid blade analysis provides less thrust than the elastic blade analysis at the same input collective. The 1-to-2-degree difference in collective for $C_T/\sigma = 0.115$ is significant for control system design. Figure 4 is a plot of rotor figure of merit (FM) vs C_T/σ for these cases with both rigid blade and elastic blade analyses. For both analyses, the peak FM is at a C_T/σ of approximately 0.175 (the airfoil design C_T/σ). The maximum FM with the elastic blade analysis is 0.625 and occurs at $C_T/\sigma = 0.179$. The maximum FM for rigid blade analysis is 0.635 and occurs with at $C_T/\sigma = 0.177$. For both analysis methods, the decrease in FM around C_T/σ of 0.20 corresponds to a sharp increase in mean drag coefficient (c_{do}), as shown in Fig. 5. This suggests significant stall on the rotor disk around and beyond this value of C_T/σ. The fact that the c_{do} values for the two analyses are approximately the same suggests that the differences in FM are due to differences in the radial distributions of lift and inflow.

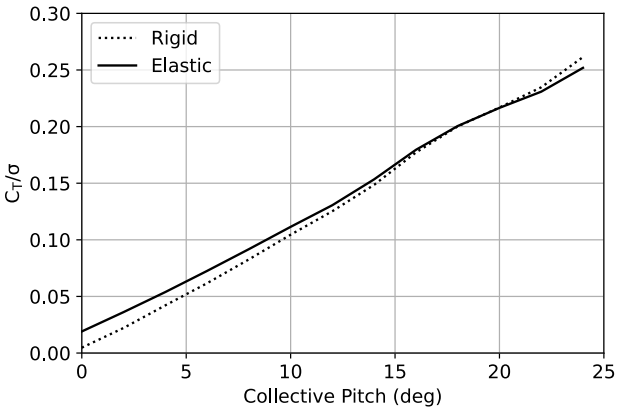

Figure 3. C_T/σ vs collective pitch, M_{tip} = 0.70

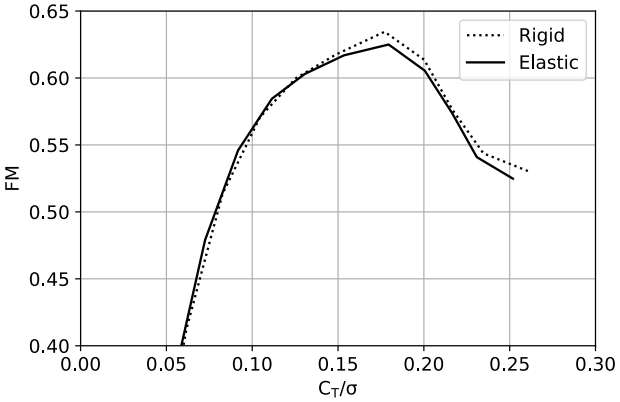

Figure 4. FM vs C_T/σ, M_{tip} = 0.70

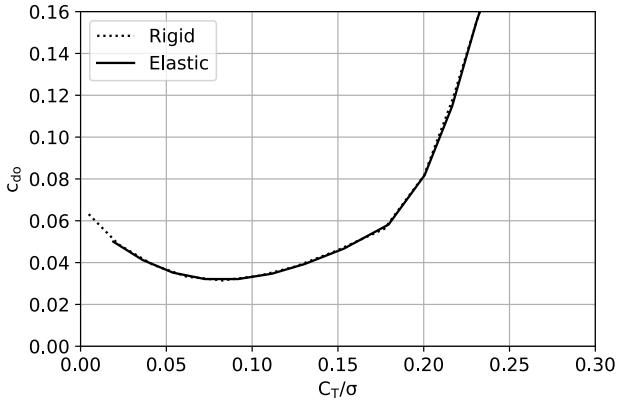

Figure 5. c_{do} vs C_T/σ, M_{tip} = 0.70

Figures 6-8 are M_{tip} = 0.80 analogs of Figs. 3-5. Figure 6 is a plot of C_T/σ vs input rotor collective pitch for both rigid and elastic blade analyses. As with the M_{tip} = 0.70 cases, from 0 to about 20 degrees collective, the rigid blade analysis provides less thrust than the elastic blade analysis at the same input collective. Figure 7 is a plot of FM vs C_T/σ for these cases with both rigid blade and elastic blade analyses. The maximum FM for elastic blade analysis is 0.625 and occurs at $C_T/\sigma = 0.187$. The maximum FM for rigid blade analysis is 0.633 and occurs at $C_T/\sigma = 0.182$. These values of FM are nearly identical to those from the M_{tip} = 0.70 cases; however, at the higher speed, the maximum FM occurs at a slightly

higher value of C_T/σ. As with the M_{tip} = 0.70 cases, the decrease in FM around C_T/σ of .20 corresponds to a sharp increase in c_{do}, as shown in Fig. 8, suggesting significant stall at this thrust level.

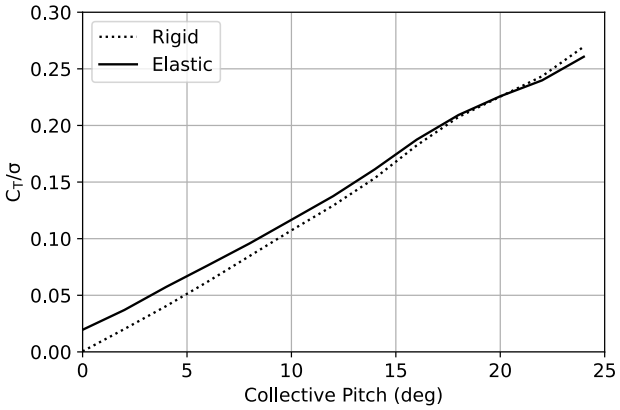

Figure 6. C_T/σ vs collective pitch, M_{tip} = 0.80

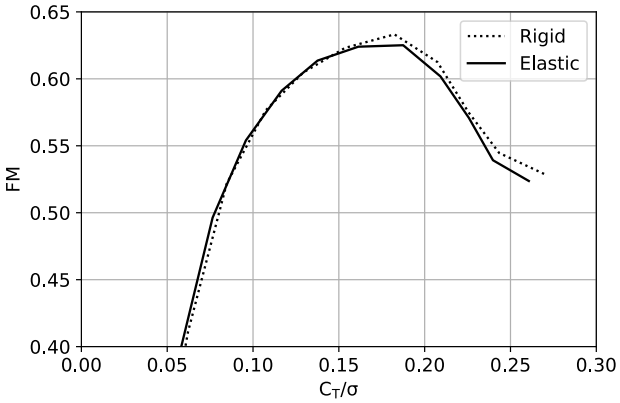

Figure 7. FM vs C_T/σ, M_{tip} = 0.80

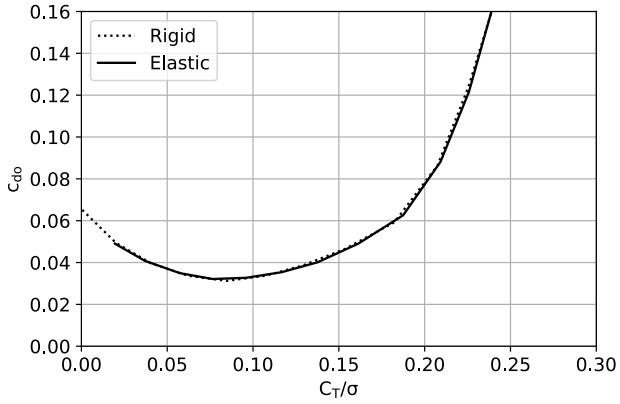

Figure 8. c_{do} vs C_T/σ, M_{tip} = 0.80

Figures 9-11 are for cases analyzed with M_{tip} = 0.90. Figure 9 is a plot of C_T/σ vs input rotor collective pitch for both rigid and elastic blade analyses. Similar to the M_{tip} = 0.70 and 0.80 cases, from 0 to nearly 20 degrees collective, the rigid blade analysis provides less thrust than the elastic blade analysis at the same input collective. Figure 10 is a plot of FM vs C_T/σ for these cases with both rigid blade and elastic blade analyses. For both analyses, the peak FM is at C_T/σ of approximately 0.175 (the airfoil design C_T/σ). The maximum FM for elastic blade analysis is 0.623 and occurs at C_T/σ = 0.170. The maximum FM for rigid blade analysis is 0.626 and occurs at C_T/σ = 0.160. For both analysis methods, the maximum FM and corresponding C_T/σ are lower for M_{tip} = 0.90 than for either M_{tip} = 0.70 or 0.80. Again, the decrease in FM around C_T/σ of 0.20 corresponds to an increase in c_{do} (suggestive of stall), as shown in Fig. 11.

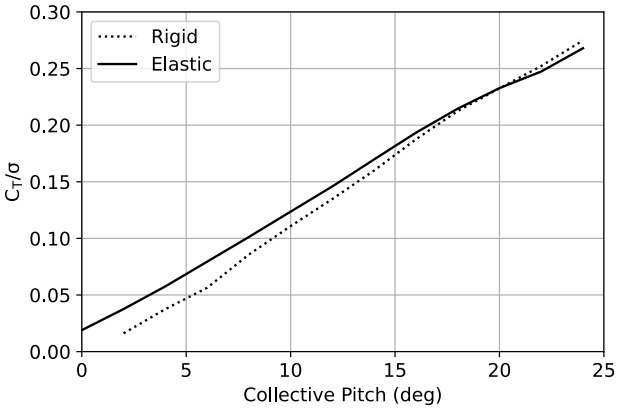

Figure 9. C_T/σ vs collective pitch, M_{tip} = 0.90

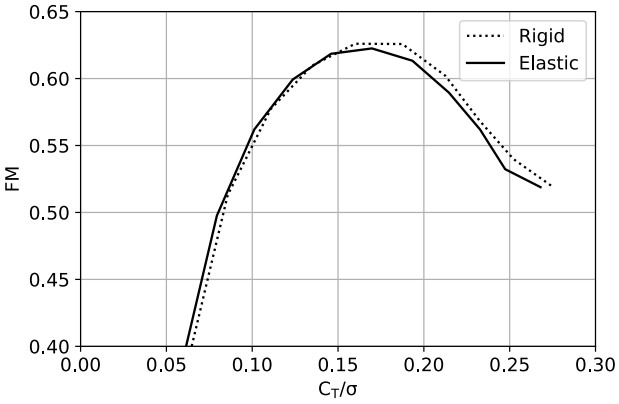

Figure 10. FM vs C_T/σ, M_{tip} = 0.90

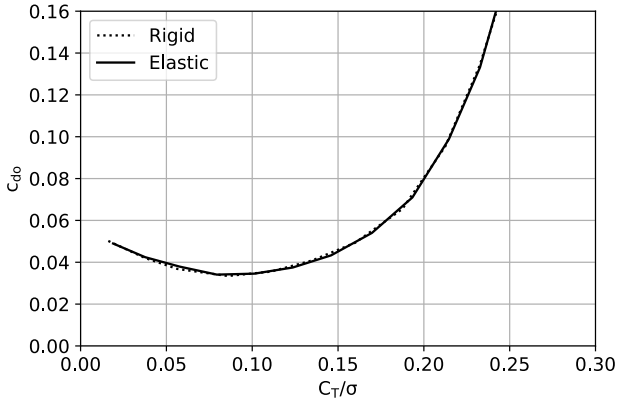

Figure 11. c_{do} vs C_T/σ, M_{tip} = 0.90

Figures 12-14 are for cases with M_{tip} = 0.95. Figure 12 is a plot of C_T/σ vs input rotor collective pitch for both rigid and elastic blade analyses. Similar to the M_{tip} = 0.70, 0.80, and 0.90 cases, from 0 degrees to nearly 20 degrees collective, the rigid blade analysis provides less thrust than the elastic blade analysis at the same input collective. Figure 13 is a plot of FM vs C_T/σ for these cases with both rigid blade and elastic blade analyses. The maximum FM for elastic blade analysis is 0.614 and occurs with at C_T/σ = 0.173. The maximum FM for rigid blade analysis is 0.619 and occurs with at C_T/σ = 0.163. For both the rigid and elastic models, the peak figure of merit decreases with M_{tip}. As with other cases, FM trails off around a C_T/σ of 0.20, corresponding with an increase in c_{do} (Fig. 14), which is indicative of stall.

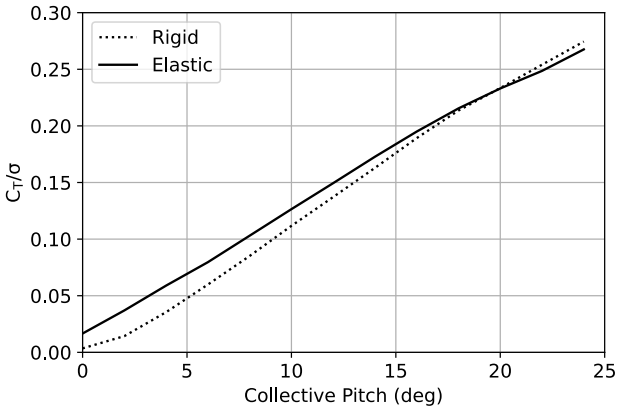

Figure 12. C_T/σ vs collective pitch, M_{tip} = 0.95

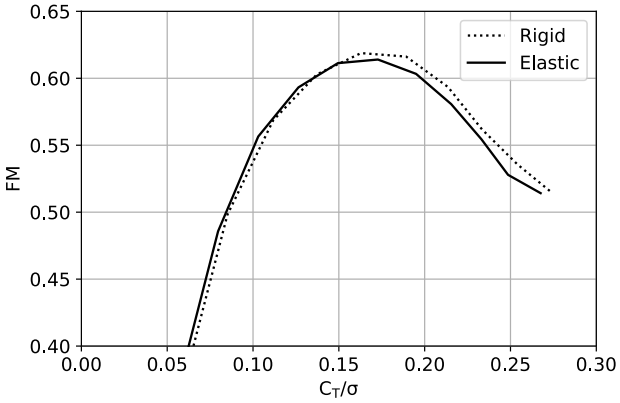

Figure 13. FM vs C_T/σ, M_{tip} = 0.95

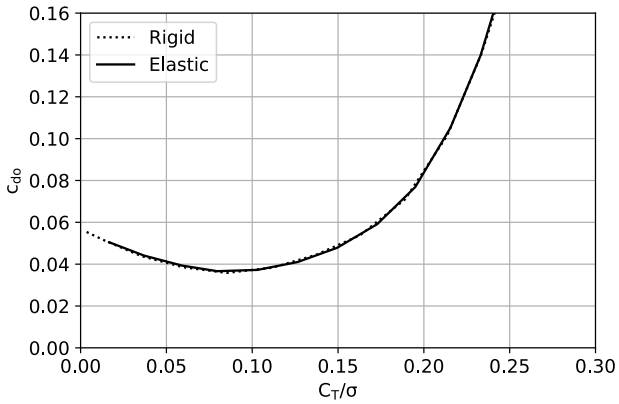

Figure 14. c_{do} vs C_T/σ, M_{tip} = 0.95

Table 3 summarizes the results of the collective sweeps for both analysis methods at the analyzed values of M_{tip}. For both analysis methods, maximum FM decreases with increasing M_{tip} (except for M_{tip} = 0.70 and 0.80, which have nearly identical FM values). There is less of a clear trend for the C_T/σ values that yield maximum FM. The third column of Table 3 lists the collective values that yield C_T/σ = 0.115 (collective values interpolated from results).

Table 3. Summary of Collective Sweep Results

M_{tip}	Max. FM	C_T/σ for max. FM	Collective (deg) for C_T/σ = 0.115
		ELASTIC	
0.70	0.625	0.179	10.369
0.80	0.625	0.187	9.840
0.90	0.623	0.170	9.230
0.95	0.614	0.173	9.022
		RIGID	
0.70	0.635	0.177	11.009
0.80	0.633	0.182	10.700
0.90	0.626	0.160	10.348
0.95	0.619	0.163	10.258

The effect on performance of elasticity for these cases is not particularly great. The maximum FM values are consistently higher for the rigid blade analysis, but by a small amount (0.5% to 1.6% higher). The most notable difference between analysis methods is seen in plots of C_T/σ vs collective pitch at low collective. Here, elastic blade analysis predicts noticeably less collective than the rigid blade analysis for the same thrust. However, for the targeted thrust value (C_T/σ = 0.175), the difference in collective between the two analysis methods is reduced. Ultimately, the results of this section suggest that blade elasticity does impact performance, but the impact is mild enough for the PAL testing to be a suitable analog for Mars operation.

Rotor Speed Sweeps

For the second set of simulations, collective pitch was fixed at four different values, (10, 18.5, 20, and 5 degrees) and rotor speed was swept from 1000 RPM to 4400 RPM (corresponding to a tip Mach number range of 0.22 to 0.97).

Figures 15-17 are plots of results for cases with collective set to 10 degrees (the collective that results in the design thrust). C_T/σ values are plotted against M_{tip} in Fig. 15 for both rigid and elastic blade analyses. Elastic analysis predicts the higher thrust value for nearly the entire range of rotor speeds, with the difference between the elastic and rigid analyses increasing with increasing rotor speed. Figure 16 is a plot of FM vs M_{tip} and shows that elastic blade analysis generally predicts better performance, particularly at higher M_{tip}. Figure 17 is a plot of c_{do} vs M_{tip} for both rigid and elastic blade analyses. Drag values for the two analysis methods are nearly identical.

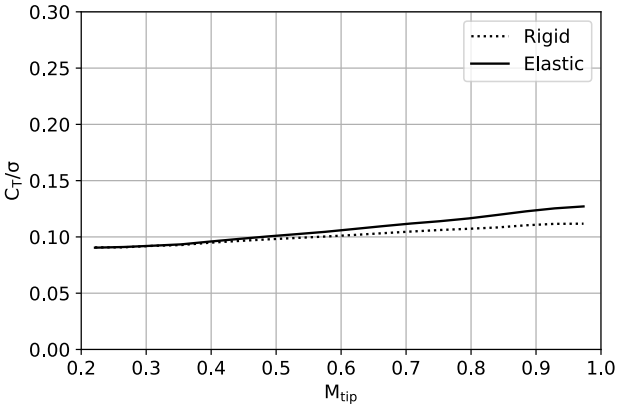

Figure 15. C_T/σ vs M_{tip}, collective = 10 degrees

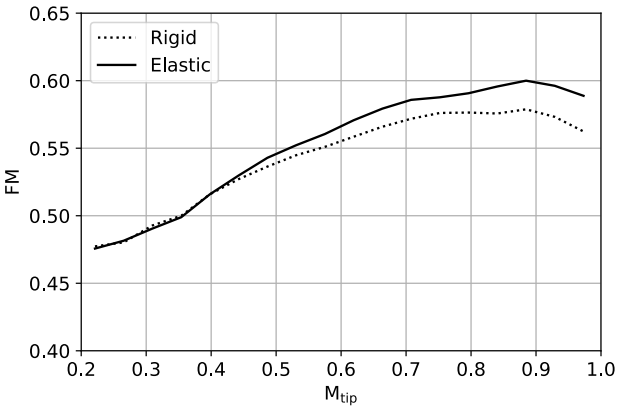

Figure 16. FM vs M_{tip}, collective = 10 degrees

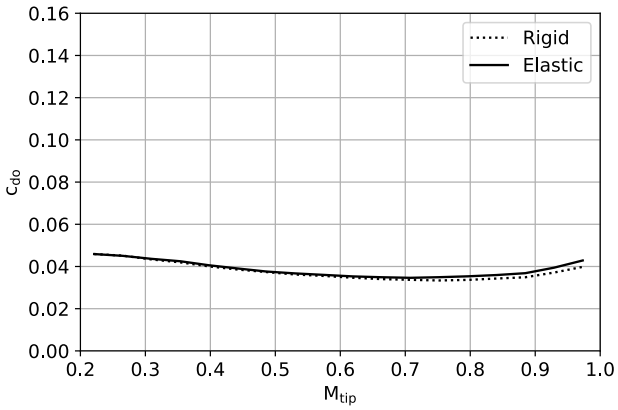

Figure 17. c_{do} vs M_{tip}, collective = 10 degrees

For collective pitch of 18.5 (the optimized value), C_T/σ values are plotted against M_{tip} in Fig. 18 for both rigid and elastic blade analyses. The two analysis methods produce very similar results, with rigid analysis predicting the higher thrust value below about M_{tip} of 0.60 and elastic blade analysis predicting the higher thrust above this M_{tip}. Figure 19, a plot of FM vs M_{tip}, shows that unlike with 10 degrees collective, the rigid blade analysis predicts better FM at higher speeds. Figure 20 is a plot of c_{do} vs M_{tip} for 18.5 degrees of collective for both rigid and elastic blade analyses. For both analysis methods, the drag is sufficiently high to conclude that the plateauing of C_T/σ beyond M_{tip} ~0.8 in Fig. 18 is due to stall. Drag is higher for rigid blade analysis until M_{tip} of about 0.75, beyond which the elastic blade analysis predicts higher drag.

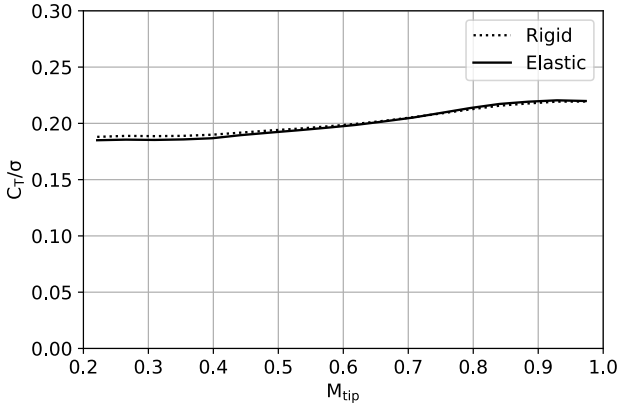

Figure 18. C_T/σ vs M_{tip}, collective = 18.5 degrees

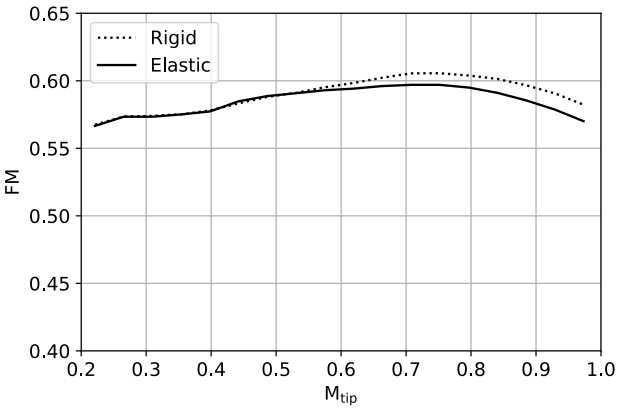

Figure 19. FM vs M_{tip}, collective = 18.5 degrees

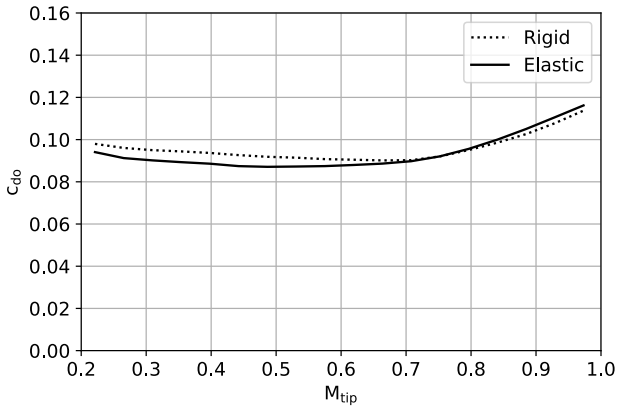

Figure 20. c_{do} vs M_{tip}, collective = 18.5 degrees

Figures 21-23 are for cases with collective set to 20 degrees. C_T/σ values are plotted against M_{tip} in Fig. 21 for both rigid and elastic blade analyses. As with the 18.5-degree collective cases, the two analysis methods produce very similar results. Rigid analysis predicts the higher thrust value below about M_{tip} of 0.65, and elastic blade analysis predicts the higher thrust above this M_{tip}. Figure 22, a plot of FM vs M_{tip}, shows close agreement between the FM predictions of the two analysis methods. Elastic blade analysis predicts slightly higher FM at lower tip speeds, while rigid blade analysis predicts higher FM at higher tip speeds. Figure 23 is a plot of c_{do} vs M_{tip} for both rigid and elastic blade analyses. As with the 18.5-degree collective cases, for both analysis methods, the drag is sufficiently high to conclude that the plateauing of C_T/σ beyond M_{tip} ~0.8 in Fig. 21 is due to stall. Drag is higher for rigid blade analysis throughout the full range of analyzed speeds.

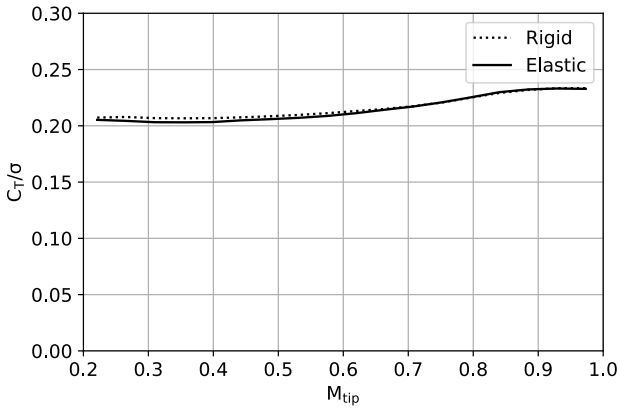

Figure 21. C_T/σ vs M_{tip}, collective = 20 degrees

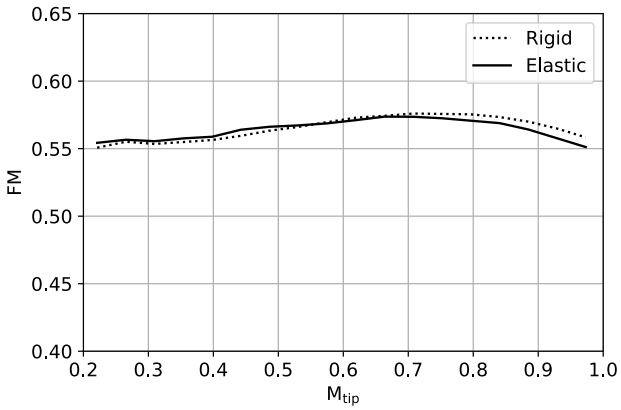

Figure 22. FM vs M_{tip}, collective = 20 degrees

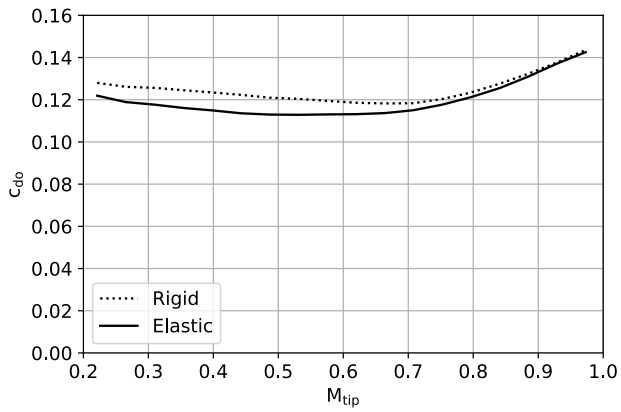

Figure 23. c_{do} vs M_{tip}, collective = 20 degrees

Figures 24-26 are plots of results for cases with collective set to a lower value, 5 degrees. C_T/σ values are plotted against M_{tip} in Fig. 24 for both rigid and elastic blade analyses. Elastic analysis predicts the higher thrust for the entire range of rotor speeds, with the difference between the elastic and rigid analyses increasing with increasing rotor speed (similarly to the 10-degree-collective cases). Figure 23 is a plot of FM vs M_{tip} for both analysis methods. For the analyzed range of speeds, the elastic blade analysis predicts higher FM than the rigid blade analysis. Note that the scale of this plot is adjusted from that of analogous plots at different collectives. This was done to capture the lower range of FM

values predicted at the 5-degree-collective, low thrust condition. Figure 26 is a plot of c_{do} vs M_{tip} for both rigid and elastic blade analyses. As with the 10-degree cases, drag values for the two analyses methods are nearly identical and far lower than for the higher collective cases.

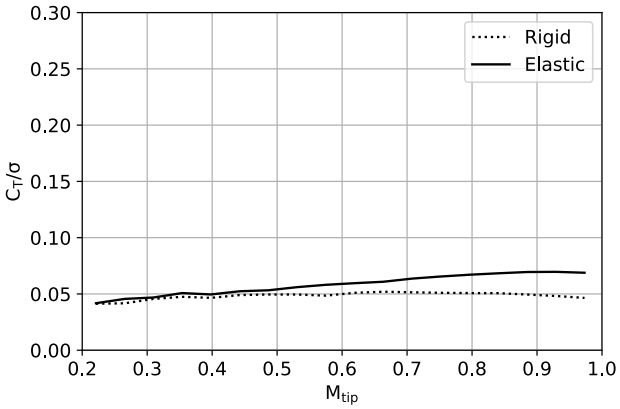

Figure 24. C_T/σ vs M_{tip}, collective = 5 degrees

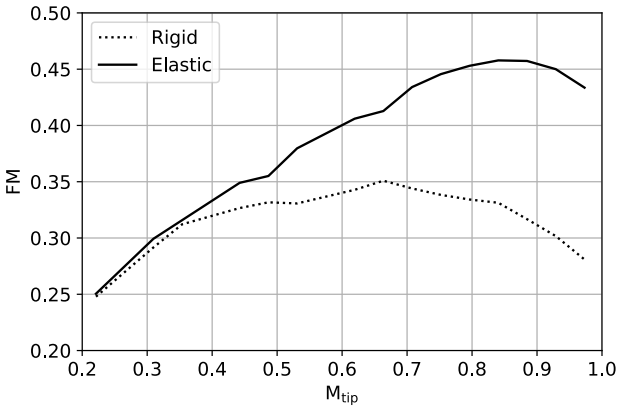

Figure 25. FM vs M_{tip}, collective = 5 degrees

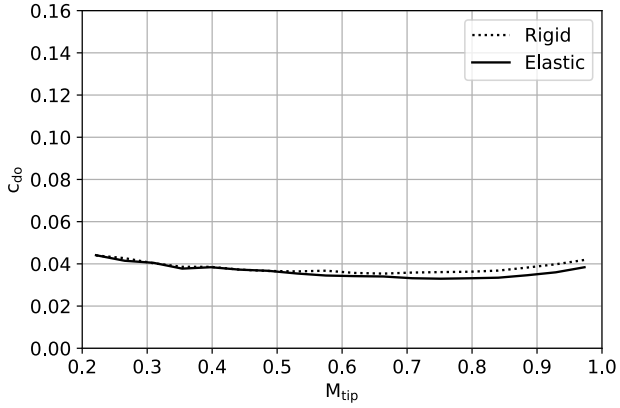

Figure 26. c_{do} vs M_{tip}, collective = 5 degrees

Overall, for the fixed collective M_{tip} sweeps, the results do not show a great deal of sensitivity to the inclusion of blade elasticity in the analysis. At the tip speeds of primary interest (above $M_{tip} = 0.70$), thrust predictions were nearly identical for the two analysis methods at the two highest collectives analyzed (18.5 and 20 degrees). For the low collective cases (5 and 10 degrees), the rigid blade analysis underpredicted the elastic analysis for C_T/σ and c_{do} for almost every analyzed speed, although in most cases, the difference was minimal. The most notable difference between analysis methods was with low collective (5 and 10 degrees) at high tip speed, a condition for which the elastic blade analysis predicted significantly more thrust than the rigid blade analysis.

CONCLUSIONS AND FUTURE WORK

Overall conclusions for this work are summarized here.

1. For the collective pitch sweeps, both rigid and elastic blade analyses show decreases in the maximum FM with increasing M_{tip} (except for $M_{tip} = 0.70$ and 0.80, which have nearly identical FM values). The most notable difference between the rigid blade and elastic blade analysis methods is at low collective, a condition at which the elastic blades require noticeably less collective than the rigid blades to reach the same thrust.
2. For the M_{tip} sweeps, the tip speeds of primary interest (above $M_{tip} = 0.70$), yielded C_T/σ and c_{do} predictions that were nearly identical for the two analysis methods at the two highest collectives analyzed (18.5 and 20 deg). For these highest collective settings, elastic analysis predicted lower FM than rigid analysis at the tip speeds of primary interest (above $M_{tip} = 0.70$).
3. The results suggest that blade elasticity does influence rotor performance in the operating conditions of interest, although the effect is moderate enough to conclude that testing in the NASA Ames Research Center Planetary Aeolian Laboratory (PAL) will be a good simulation of Mars operation.

There is a continuing effort to determine blade section structural properties more precisely using 2D finite-element analysis. Once this modelling effort is successfully completed, the analysis presented in this work will be updated with the new blade properties. Additionally, experimental methods for obtaining section stiffness properties are being explored. If these experimentally determined values become available, they will be incorporated into the CAMRAD II model.

Experimental testing of the ROAMX rotor is currently planned for early 2023. Once experimental results are obtained, they will be compared with the computational predictions.

Author contact:
Stephen J. Wright stephen.j.wright@nasa.gov
Witold J. F. Koning witold.koning@nasa.gov
B. Natalia Perez Perez natalia.perezperez@nasa.gov
Haley V. Cummings haley.cummings@nasa.gov
Wayne Johnson wayne.johnson@nasa.gov

ACKNOWLEDGMENTS

The authors acknowledge the support of members of the NASA Ames Research Center Rotorcraft Aeromechanics Office. In particular, thanks go to Chris Silva for his guidance with the IXGEN/VABS software and to William Warmbrodt for his guidance and mentorship. Funding for the ROAMX project is through the NASA Space Technology Mission Directorate Early Career Initiative.

REFERENCES

1. Cummings H. V., et. al., "Overview and Introduction of the Rotor Optimization for the Advancement of Mars eXploration (ROAMX) Project," VFS Aeromechanics for Advance Vertical Flight Technical Meeting, San Jose, CA, January 25-27, 2022.

2. Koning, W. J. F., Romander, E. A., and Johnson, W., "Optimization of Low Reynolds Number Airfoils for Martian Rotor Applications Using an Evolutionary Algorithm," AIAA Paper NO. 2020-0084, January 2022.

3. Lumba, R., Cheng, C., Datta, A., "Structural Design and Aeromechanical Analysis of Unconventional Blades for Future Mars Rotorcraft," VFS Aeromechanics for Advanced Vertical Flight Technical Meeting, San Jose, CA, January 25-27, 2022.

4. "Planetary Aeolian Laboratory" [Online]. Available: https://www.nasa.gov/ames/planetary-aeolian-laboratory. [Accessed: 10-Jan-2023].

5. Grip, H. F., et al., "Modeling and Identification of Hover Flight Dynamics for NASA's Mars Helicopter," Journal of Guidance, Control, and Dynamics, Vol. 43, No. 2, February 2020.

6. Johnson, W., "Rotorcraft Aeromechanics Applications of a Comprehensive Analysis," HeliJapan 1998: AHS International Meeting on Rotorcraft Technology and Disaster Relief, Gifu, Japan, April 1998.

7. Rohl, P. J., Cesnik, C. E. S., Dorman, P., Kumar, D., "IXGEN – A Modeling Tool for the Preliminary Design of Composite Rotor Blades," AHS Future Vertical Lift Aircraft Design Conference, San Francisco, CA, January 18-20, 2012.